Godunov Finite-Volume for Multi-lane Highway Modeling

Shraman Ray Chaudhuri

February 26, 2017

1 Overview

This project is an extension of Project 3 into the multi-lane highway model, along with thorough justification of procedures and parameters, investigation into interesting multi-lane traffic patterns, and more rigorous error, stability, and correctness analyses.

2 Brief Review of 1-Lane Model

In my original Project 3, I implemented a **Godunov** scheme for flux reconstruction at cell interfaces based on a 4-part characteristic analysis of the Riemann problem. The analysis is summarized below:

$\underline{\rho_L, \rho_R < 0.5}$ Both characteristics move to the right. In the case that $\rho_L < \rho_R$, the discontinuity is preserved, and otherwise dissipates as the solution translates to the right. In either case, the flux at the interface tends to $f(\rho_L)$.

$\underline{\rho_L, \rho_R > 0.5}$ Both characteristics move to the left. In the case that $\rho_L < \rho_R$, the discontinuity is preserved, and otherwise dissipates as the solution translates to the left. In either case, the flux at the interface tends to $f(\rho_R)$.

$\underline{\rho_L \leq 0.5, \rho_R \geq 0.5}$ Characteristics at the left have positive slope, whereas characteristics at the right have negative slope. Therefore, information travels into the discontinuity and the discontinuity is preserved. For consistency with the initial condition at $\rho(x = 0) = \rho_L$, we choose our flux to be $f(\rho_L)$.

$\underline{\rho_L \geq, \rho_R \leq 0.5}$ The characteristics on each side move away from the discontinuity in opposite directions. By the entropy condition, the discontinuity dissipates and we take the value of the flux to be the stationary point, i.e. the point at which $\frac{\partial f}{\partial u}$ is zero (a local maximum). The local maximum occurs at 0.5, so we have $f_{max} = f(0.5) = 0.25$.

For the solution reconstruction, I chose the **vanLeer** flux limiter due to its better handling of oscillations at the interfaces and its total-variation-diminishing behavior. Below are sample plots of the solutions produced with these initial schemes:

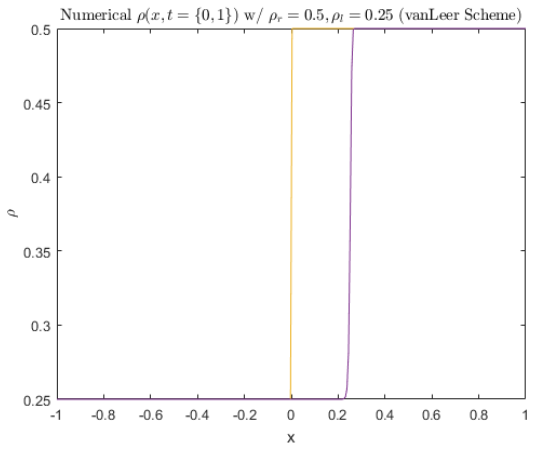

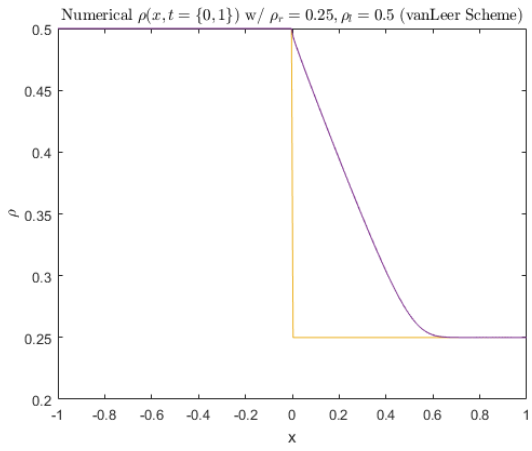

3 2-Lane Model

3.1 Derivation of 2-Lane FVM

Our governing equation for the first lane is

$$\frac{\partial \rho_1}{\partial t} + \frac{\partial f_1}{\partial x} = s_1 = \alpha(\rho_2 - \rho_1)$$

Integrating both sides of the equation over a single cell and dividing by Δx, we have

$$\frac{1}{\Delta x}\left[\int_{x_{i-\frac{1}{2}}}^{x_{i+\frac{1}{2}}} \left(\frac{\partial \rho_1}{\partial t}\right) dx + \int_{x_{i-\frac{1}{2}}}^{x_{i+\frac{1}{2}}} \left(\frac{\partial f_1}{\partial x}\right) dx\right] = \frac{1}{\Delta x}\left[\int_{x_{i-\frac{1}{2}}}^{x_{i+\frac{1}{2}}} (\alpha(\rho_2 - \rho_1))\, dx\right]$$

$$\frac{\partial}{\partial t}\frac{1}{\Delta x}\int_{x_{i-\frac{1}{2}}}^{x_{i+\frac{1}{2}}} (\rho_1)\, dx + \frac{1}{\Delta x}(f_{i+\frac{1}{2}} - f_{i-\frac{1}{2}}) = \frac{\alpha}{\Delta x}\int_{x_{i-\frac{1}{2}}}^{x_{i+\frac{1}{2}}} (\rho_2)\, dx - \frac{1}{\Delta x}\int_{x_{i-\frac{1}{2}}}^{x_{i+\frac{1}{2}}} (\rho_1)\, dx$$

$$\frac{\partial}{\partial t}\bar{\rho}_1 + \frac{1}{\Delta x}(f_{i+\frac{1}{2}} - f_{i-\frac{1}{2}}) = \alpha(\bar{\rho}_2 - \bar{\rho}_1)$$

The derivation is symmetric for lane 2.

The right-hand side indicates that in order to incorporate the new source term, we can simply incorporate a scaled difference of the cell-averaged solutions (i.e. the difference between `p_bar_1` and `p_bar_2` in the original solver code).

3.2 First-Order Reconstruction

Using a simple Godunov scheme (see `dpdt_2lane_1.m`), we get the following result for our 2-Lane problem (sampled solutions from $t = 0$ to $t = 1$):

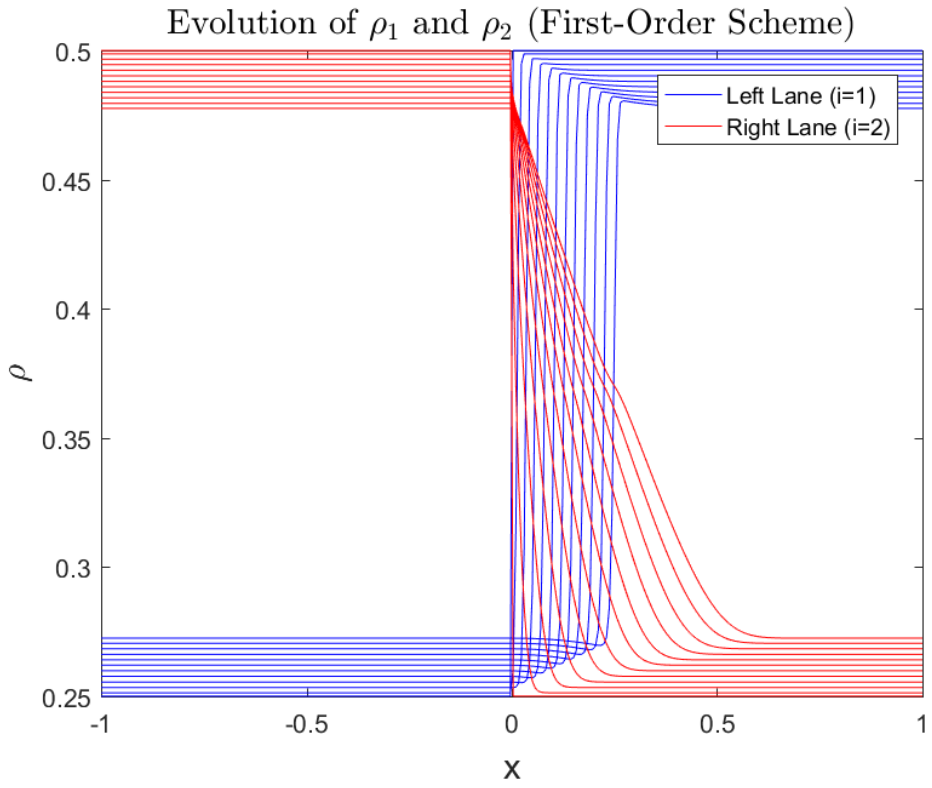

3.3 Higher-Order Reconstruction (Limiters)

We now employ a van Leer limiter as we had before, to achieve higher accuracy in our solution reconstruction. Specifically, since the van Leer limiter falls approximately in the middle of the admissibility region for flux limiters, we should expect high accuracy at both the non-smooth (2nd order accurate) and smooth (4th order accurate) regions. Below is a plot demonstrating these effects with the vanLeer limiter:

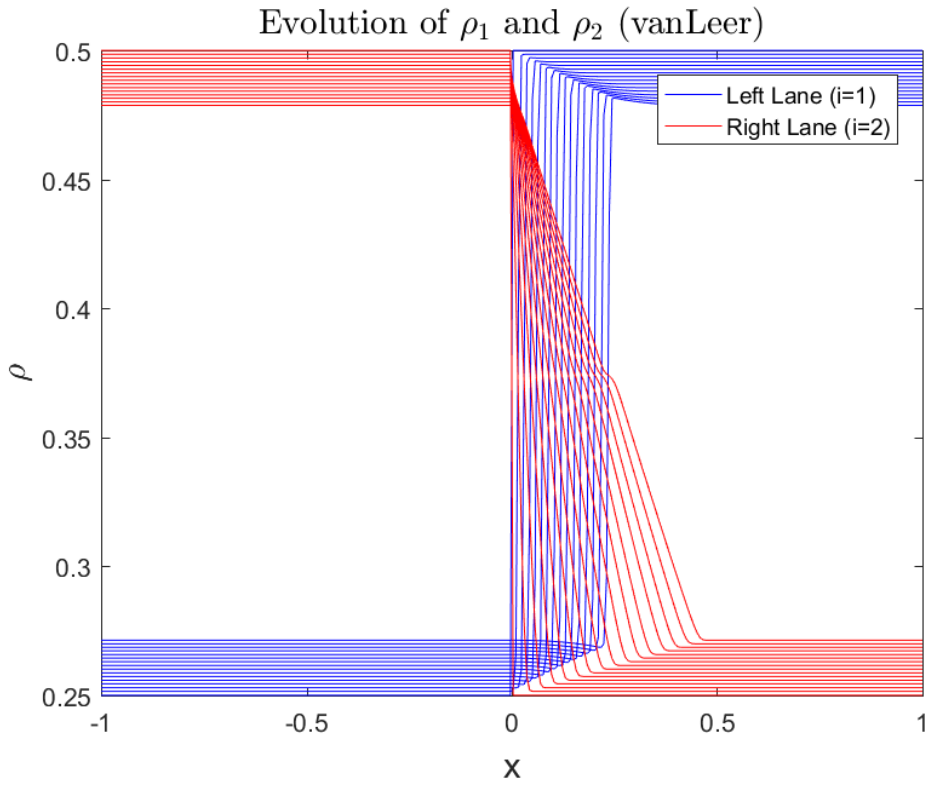

3.4 Analysis and Justification

The plots seem to fit the model both intuitively and quantitatively. The source term represents the influx/outflux of cars based on the difference in densities between adjacent lanes. In the region $x \leq 0$, the density of cars in the left lane is less than the density of cars in the right lane, so we see the density shift from the left to the right lane (i.e. cars are switching lanes to lower traffic). The opposite happens in the region $x > 0$, where the right lane density is increases and the left lane's decreases.

The difference in the shape of the two solutions can be explained by characteristic analysis at the discontinuities. In the left lane we have the shock speed $S_s = \frac{f(\rho_L)-f(\rho_R)}{\rho_L-\rho_R} > 0$, so our characteristics from the left move the discontinuity to the right and preserve it. However, in the right lane, the $x > 0$ region translates to the right whereas the $x \leq 0$ region stagnates. Therefore, to ensure our entropy condition is met (i.e. that no information comes out of the discontinuity), we see the discontinuity dissipate at the tail end of the curve. Furthermore, the characteristics at lower values have greater slope than at values closer to $\rho = 0.5$, so we see the bottom of the curve get pulled out faster than the top of the curve.

3.5 Stability

A necessary condition for stability is that the CFL condition for our explicit time-marching scheme. For the 1-dimensional case, the CFL condition requires that

$$C = \frac{u\Delta t}{\Delta x} \leq C_{max} = 1$$

This condition must be met for all u across the spatial and time domain, and ensures that an explicit time-marching algorithm has fine enough resolution with respect to the spatial discretization so that information doesn't travel past more than 1 cell in any direction. To ensure that we meet the CFL condition, we can measure the maximum velocity at any point in each lane across time and check that all maximum values meet the CFL condition. A plot of the CFL numbers across time is given below.

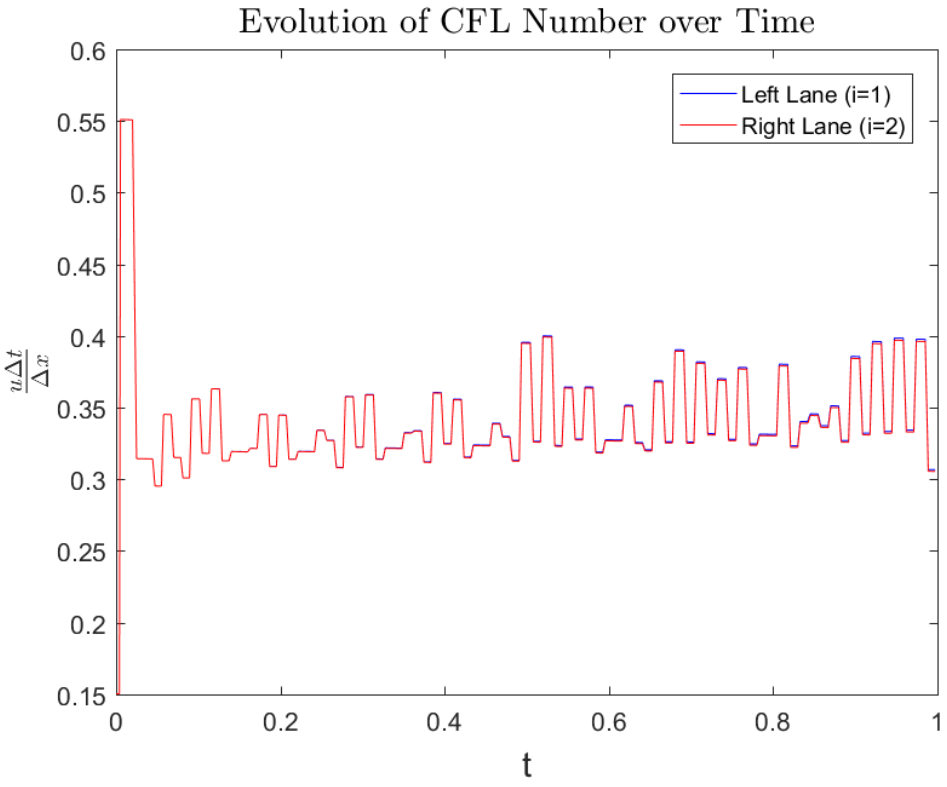

Since the CFL number never exceeds 1, we know our spatial vs. time resolution meets the first criterion for stability (necessary but not sufficient). The second criterion is to make sure that, for each lane, the total variation is indeed nonincreasing (in this case, it should diminish since there is a preserved discontinuity in the solution). The below plot shows the evolution of the total variation across time for the two lanes.

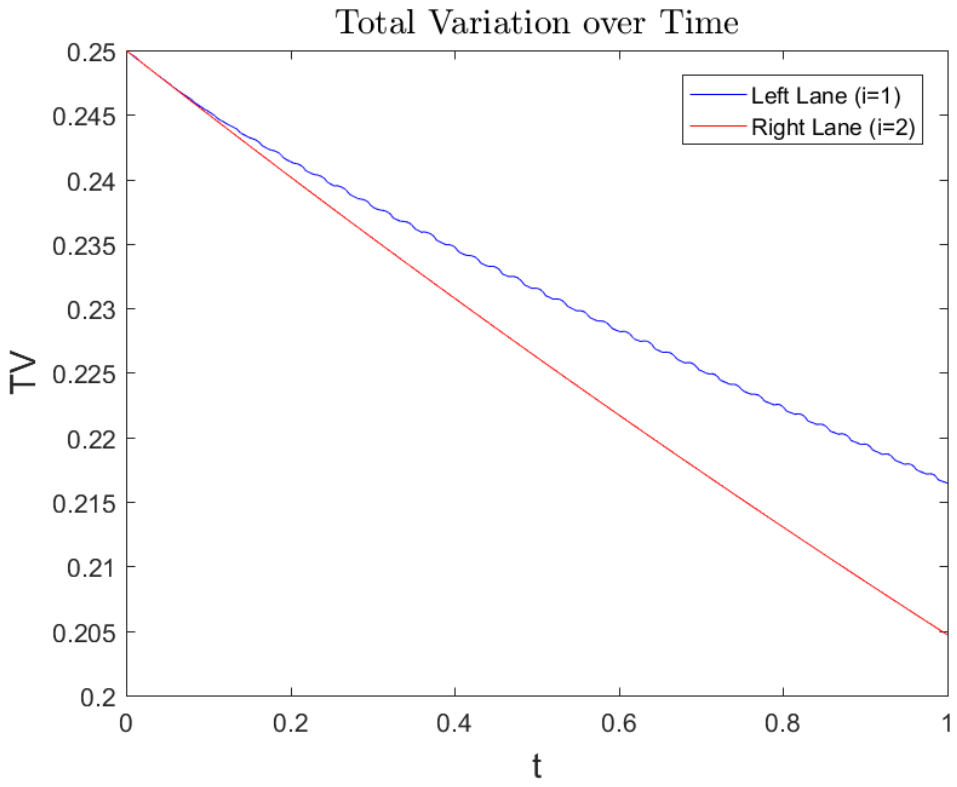

This makes sense since in both lanes, we maintain the monotonocity of the solution and do not introduce any local extrema. The total variation is therefore nonincreasing. Furthermore, we maintain conservation of traffic mass throughout our solution as the decrease in density at any point in one lane is counteracted by an increase in the other, i.e. $\int_{x_{begin}}^{x_{end}} (\rho_1 + \rho_2)dx$ is constant.

3.6 Error

Since we cannot solve the multi-lane case as easily using analytic approaches, I use an extremely fine-grained grid to gauge the "ground-truth" solution. I used several error metrics in gauging the performance of the solution, particularly the l_1 and l_2 norms (plots included below). The errors were determined by interpolating the lower resolution solution onto the higher resolution solution and dividing the total error by the number of grid points in the low-res solution.

In order to determine an appropriate grid resolution to act as a ground-truth, I increased the resolution until successive refinemenets exhibited an error epsilon of $\epsilon \leq 10^{-15}$. This epsilon is less than the machine epsilon for single-precision floating point numbers and approaches the machine epsilon for double-precision floating point numbers. The grid resolution at which this ratio was achieved was around 2000, so the "ground-truth" solution is the numerical

solution obtained with 2000 cells.

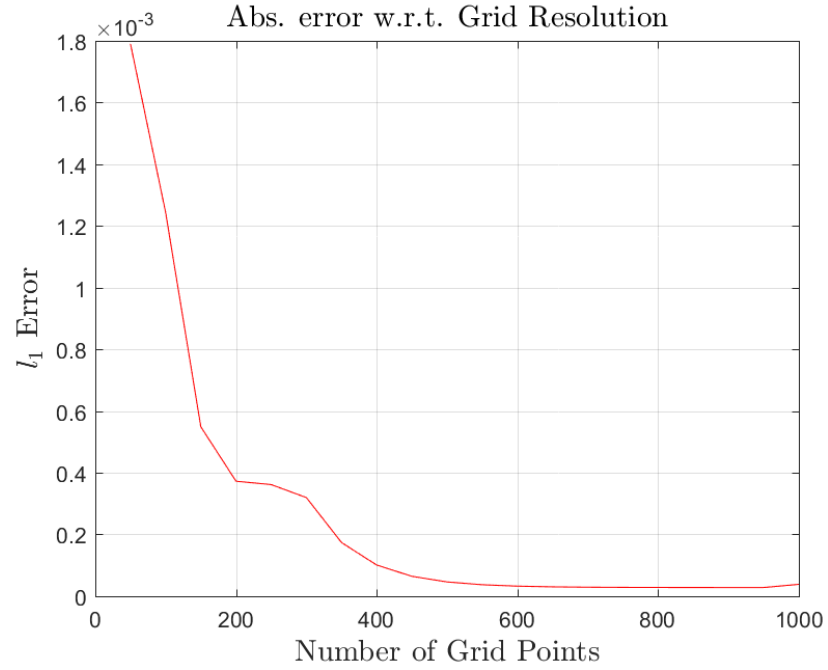

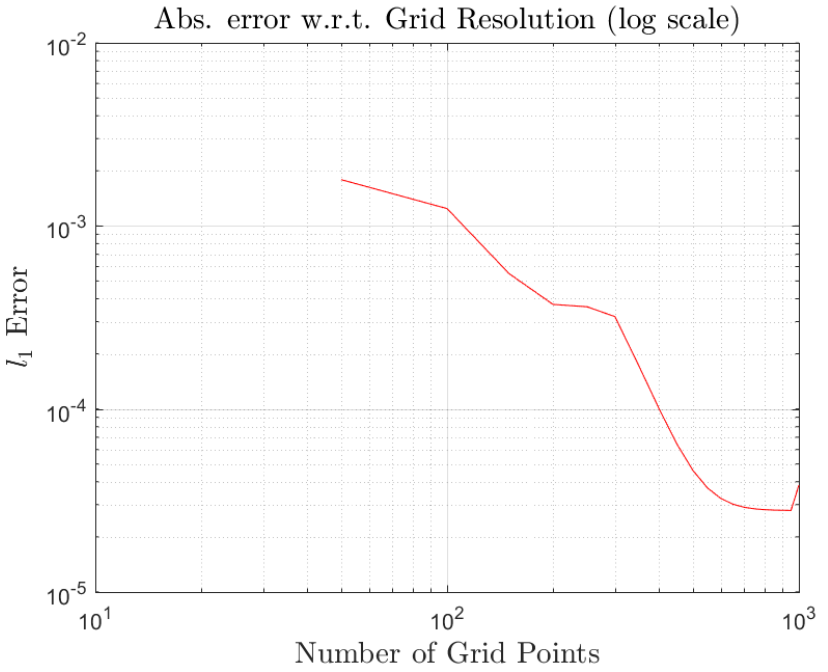

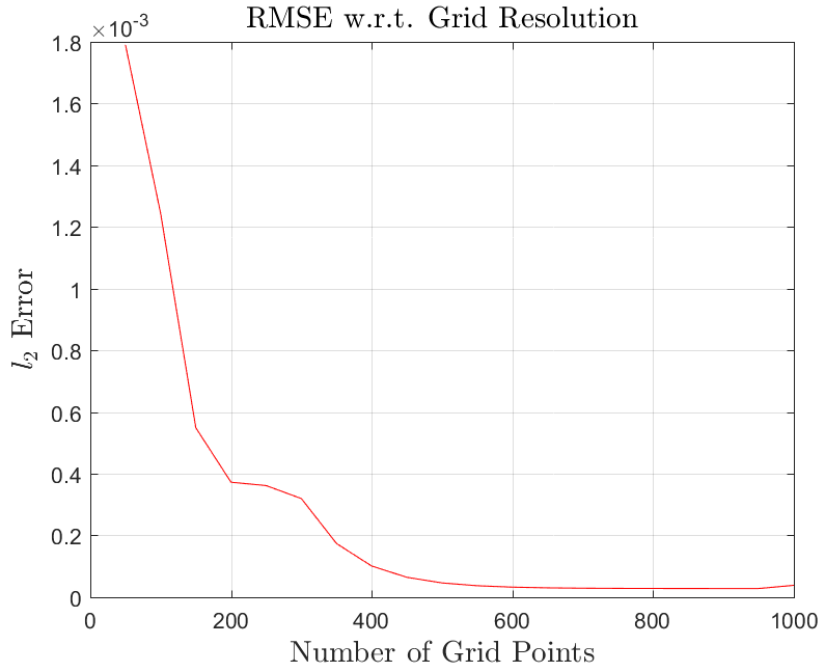

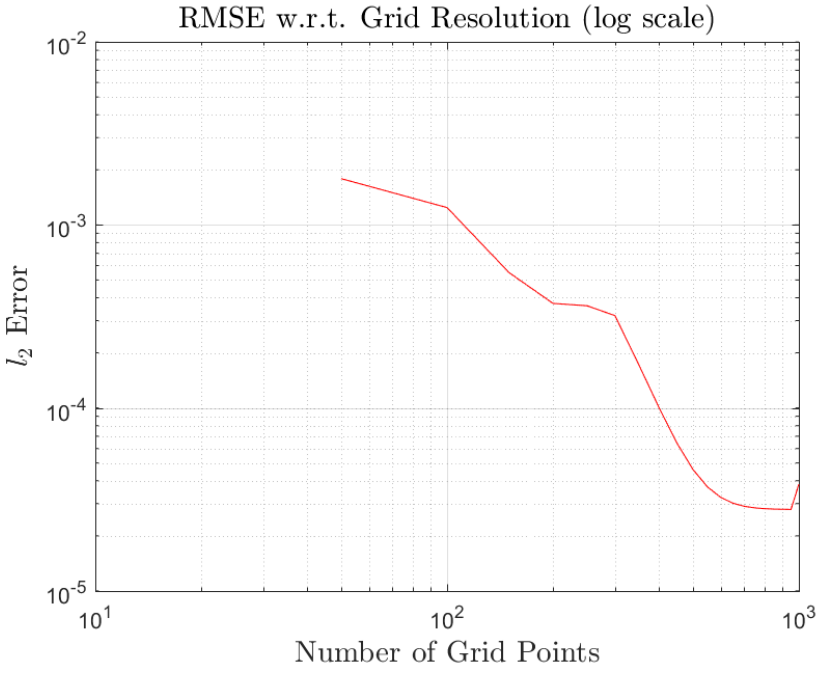

The error plots seem to suggest that the error grow on the order of approximately $O(\Delta x^{1.5})$, and the average slope tends to $O(\Delta x^2)$.

3.7 Accuracy

The **consistency** demonstrated by our decreasing error as well as the **stability** exhibited by our scheme choice are sufficient to ensure our numerical solution is **accurate**.

4 Extending to n-Lane Model

4.1 Problem Setup 1

To diversify the problem scenario a bit, I chose a more complex initial setup than the ordinary Riemann problem in Project 3. As a first test situation: for lane i, we have i concatenated Riemann problems evenly spaced over the domain, where odd lanes start with $\rho_L > \rho_R$ and even lanes start with $\rho_R > \rho_L$ at the boundaries. For this case, I use 4 lanes.

Specifically,

$$\rho_1 = \begin{cases} 0.25 & x \leq 0 \\ 0.5 & x > 0 \end{cases}$$

$$\rho_2 = \begin{cases} 0.5 & -1 \leq x \leq -0.5 \\ 0.25 & -0.5 < x \leq 0 \\ 0.5 & 0 < x \leq 0.5 \\ 0.25 & 0.5 < x \leq 1 \end{cases}$$

$$\rho_3 = \begin{cases} 0.25 & -1 \leq x \leq -0.667 \\ 0.5 & -0.667 < x \leq -0.333 \\ 0.25 & -0.333 \leq x \leq 0 \\ 0.5 & 0 < x \leq 0.333 \\ 0.25 & 0.333 < x \leq 0.667 \\ 0.5 & 0.667 < x \leq 1 \end{cases}$$

$$\rho_4 = \begin{cases} 0.5 & -1 \leq x \leq -0.75 \\ 0.25 & -0.75 < x \leq -0.5 \\ 0.5 & -0.5 < x \leq -0.25 \\ 0.25 & -0.25 < x \leq 0 \\ 0.5 & 0 < x \leq 0.25 \\ 0.25 & 0.25 < x \leq 0.5 \\ 0.5 & 0.5 < x \leq 0.75 \\ 0.25 & 0.75 < x \leq 1 \end{cases}$$

The initial condition is shown graphically below:

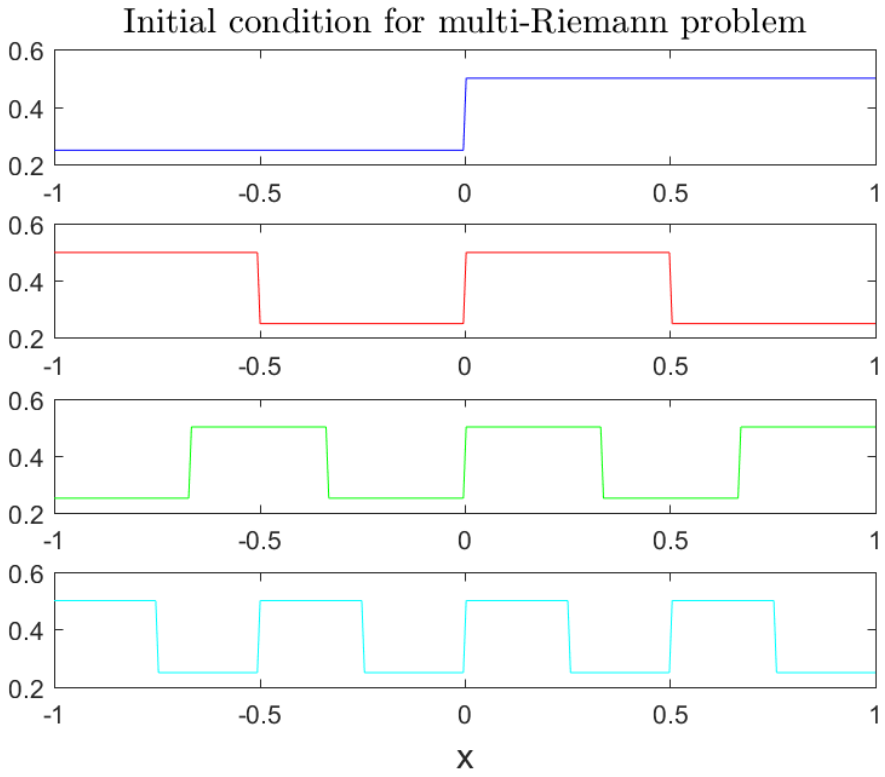

4.2 Solution Method and Analysis

The solution method is easily extensible from the derivation for the 2-Lane method. Instead of having a single source term on the right-hand side of the integral, now we have up to 2 different source terms for every lane i of the form $\bar{\rho}_{i+1} + \bar{\rho}_{i-1} - 2\bar{\rho}_i$. The solver now loops over multiple lanes instead of the fixed two lanes from before (see `dpdt_nlane.m`).

The time-evolution of the solution for Problem Setup 1 is shown below:

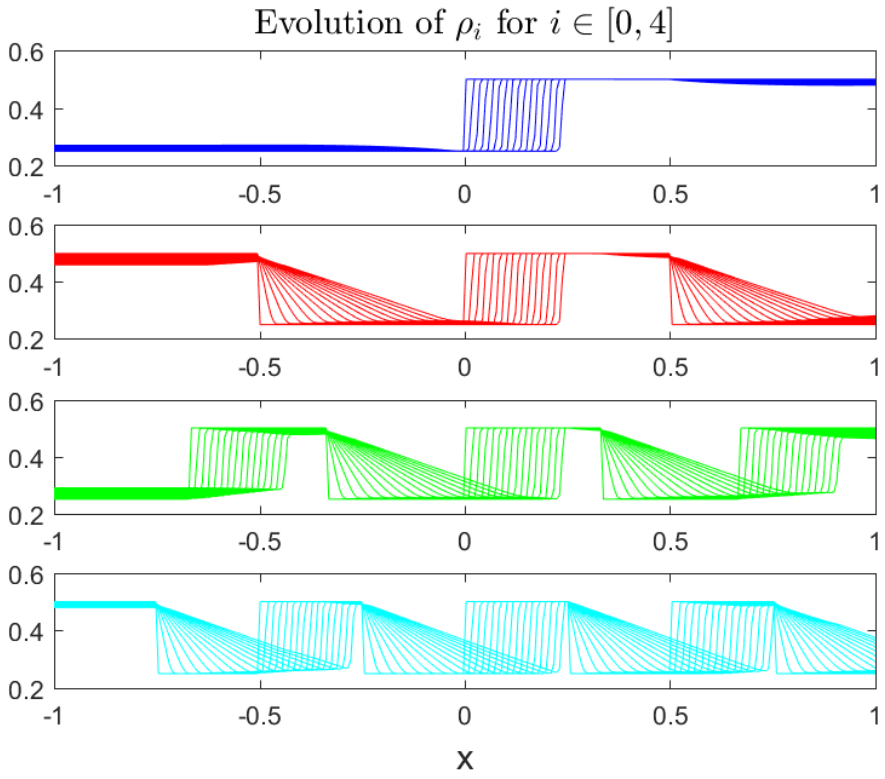

4.3 Analysis: Correctness, Error, Stability

The correctness argument follows very similarly as in the 2-lane case since we have simply extended our Riemann problem to 4 lanes. We see that the solution follows the density gradients as before, with high density regions transferring over to adjacent low density lanes. We see the same discontinuity artifacts as in the 2-lane case depending on the transition from $\rho_R \to \rho_L$ or $\rho_L \to \rho_R$ as expected.

Furthermore, we see that the total variation for the middle lanes diminish at a faster rate than the lanes at the edges (since the density gradient, i.e. source term, is amplified by having two adjacent lanes instead of one). We see all solutions tend to a steady state, where all densities will eventually be uniform.

(See following pages for error/stability analyses and plots).

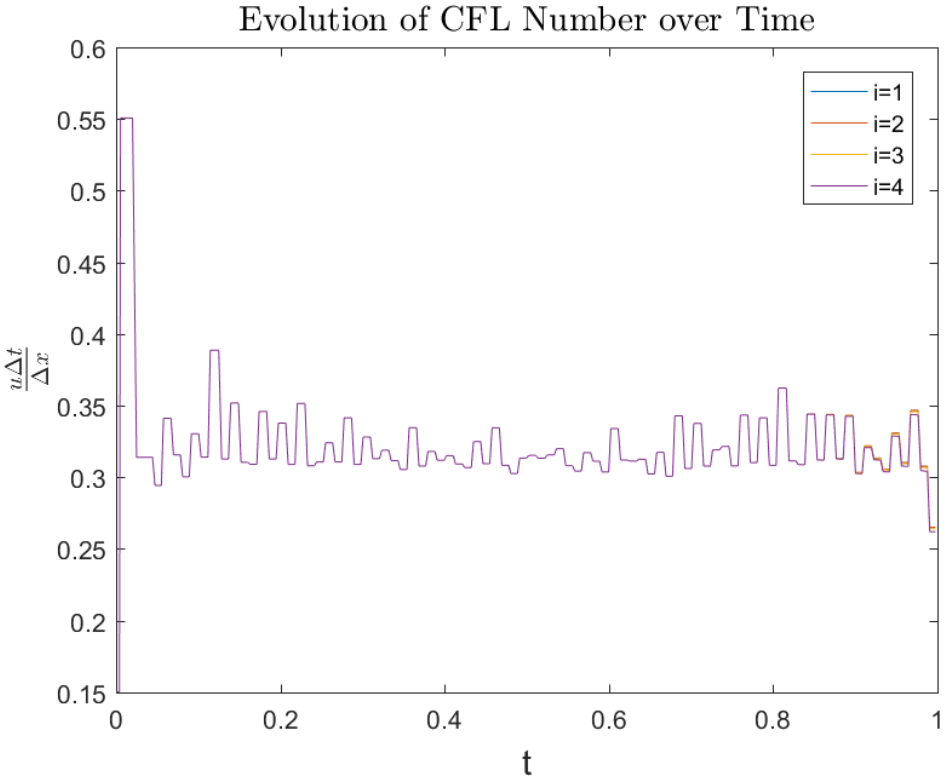
Evolution of CFL Number over Time
$\frac{u\Delta t}{\Delta x}$
t
i=1
i=2
i=3
i=4
0.6
0.55
0.5
0.45
0.4
0.35
0.3
0.25
0.2
0.15
0
0.2
0.4
0.6
0.8
1

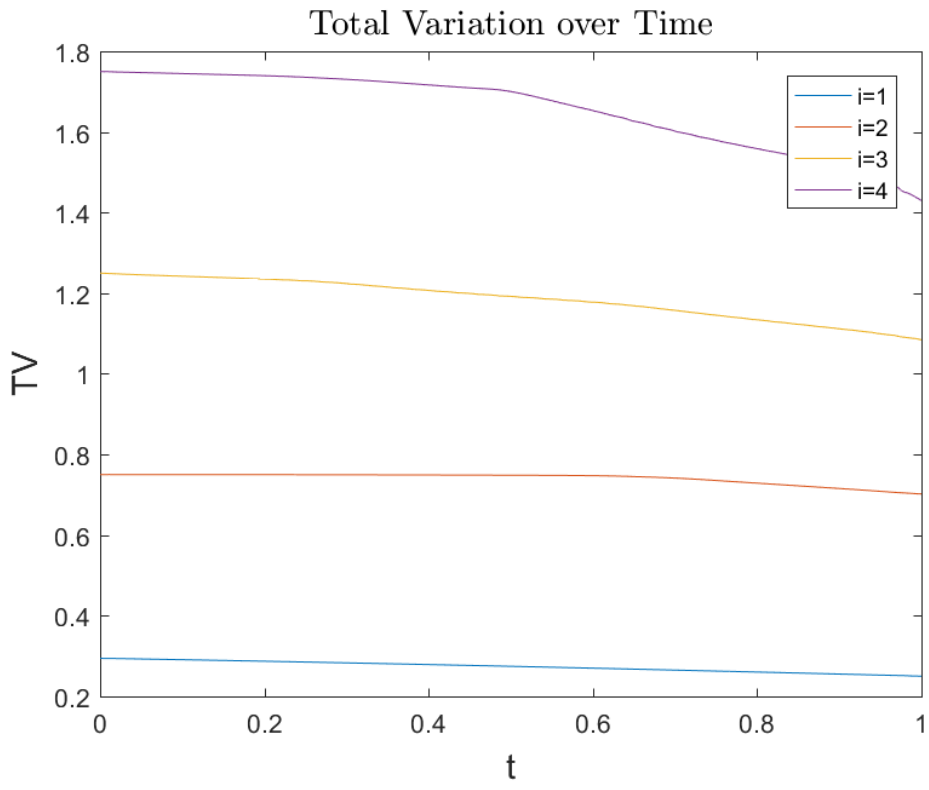
Total Variation over Time
TV
t
i=1
i=2
i=3
i=4
1.8
1.6
1.4
1.2
1
0.8
0.6
0.4
0.2
0
0.2
0.4
0.6
0.8
1

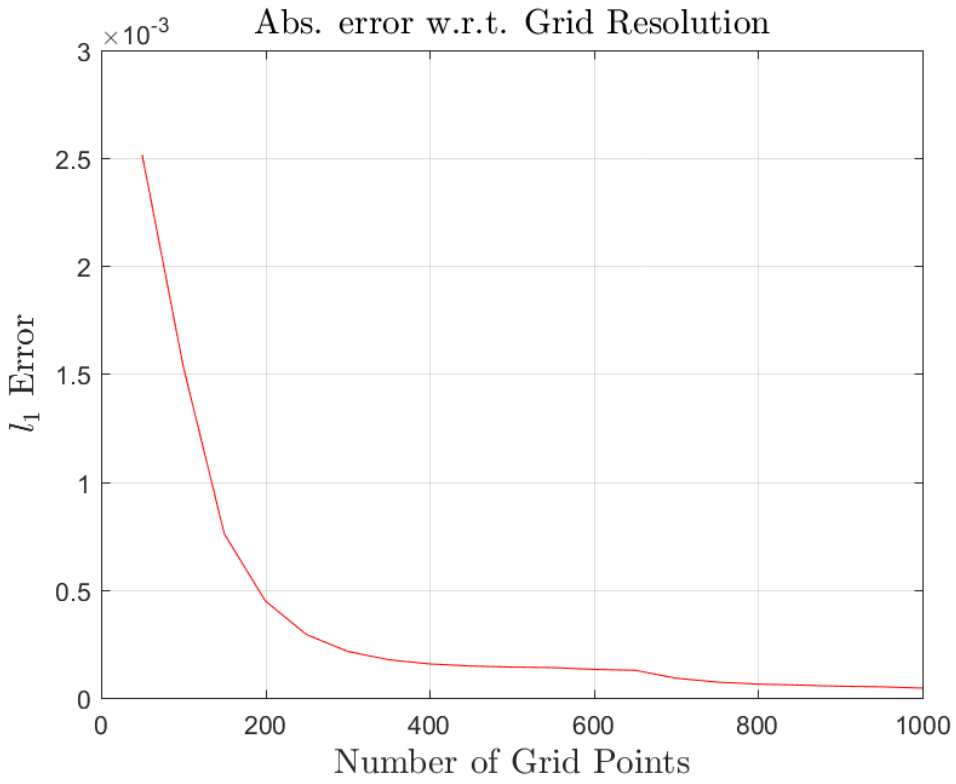
Abs. error w.r.t. Grid Resolution
×10^-3
3
2.5
2
1.5
1
0.5
0
l_1 Error
0
200
400
600
800
1000
Number of Grid Points

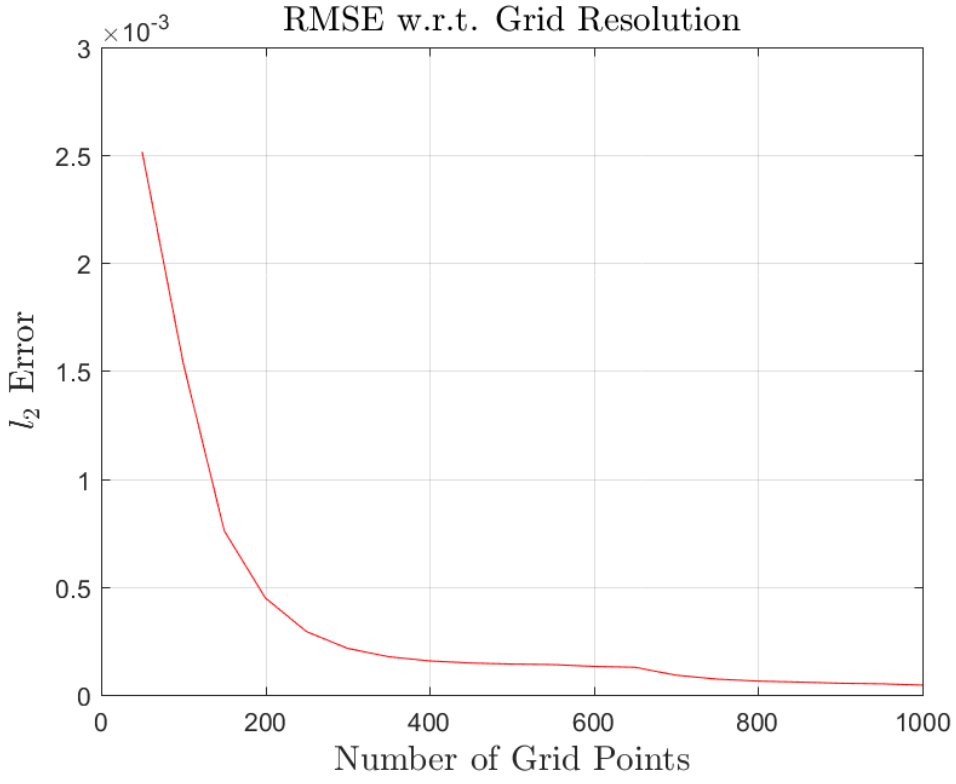
RMSE w.r.t. Grid Resolution
×10^-3
3
2.5
2
1.5
1
0.5
0
l_2 Error
0
200
400
600
800
1000
Number of Grid Points

We use the same methodologies for error analysis and stability as in the 2-lane case. The plots on the previous pages show the CFL number, the total variation of all lanes, and the error as a function of grid spacing.

As before, we see that our solution scheme meets the CFL condition and is total variation diminishing, indicating stability. The error decreases as the grid resolution increases, so our solution is consistent. Furthermore, the grid convergence rate has the same order of magnitude as in the 2-lane model. Therefore, with our stability and consistency criteria met, we argue that this numerical solution is accurate.

4.4 Problem Setup 2: Measuring the effect of α

Another interesting case would be to see how fast the traffic distributes itself out with varying values of α. As α is increased, the source term on the right-hand side of the equation should increase, eliciting more lane-changing, and therefore faster convergence to the steady state.

To measure this effect, we use a simple case where there are two densely populated lanes on the two ends and sparsely populated lanes in the middle. The initial condition for this problem setup is shown below:

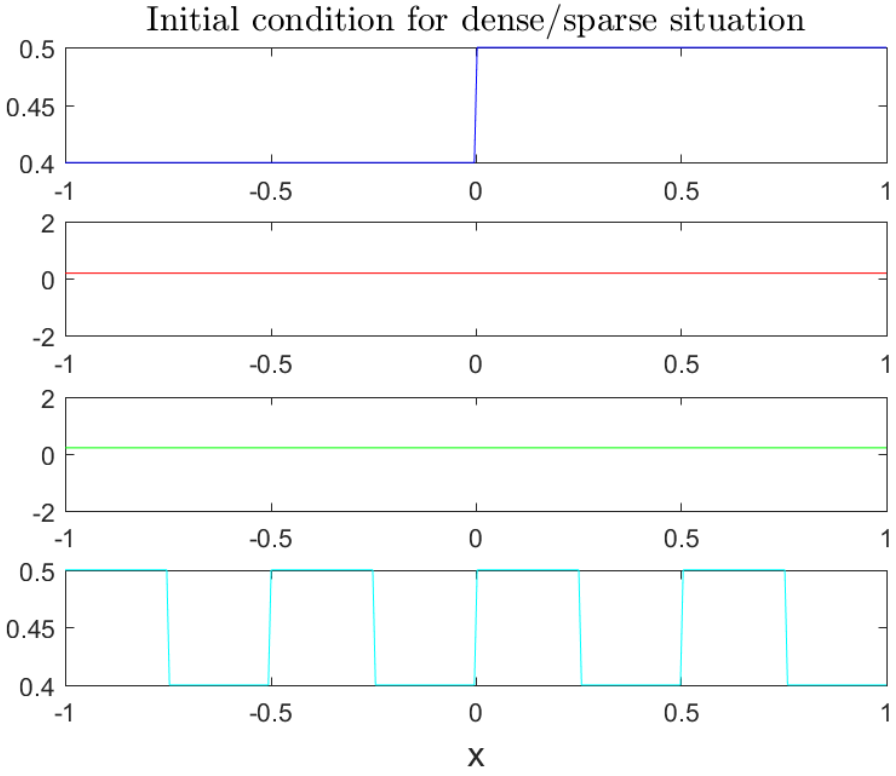

Below are plots of the time-evolution of the solution with $\alpha = 0.05$ and $\alpha = 0.5$.

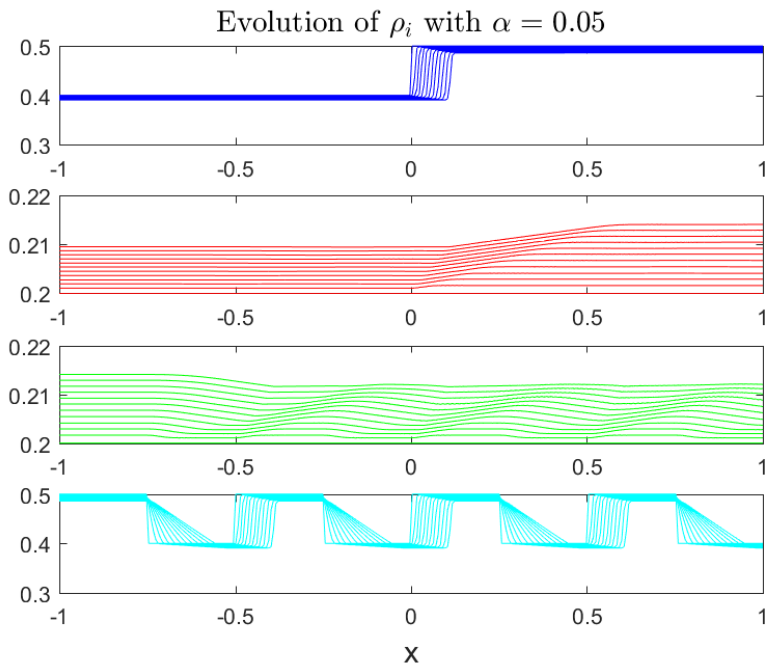

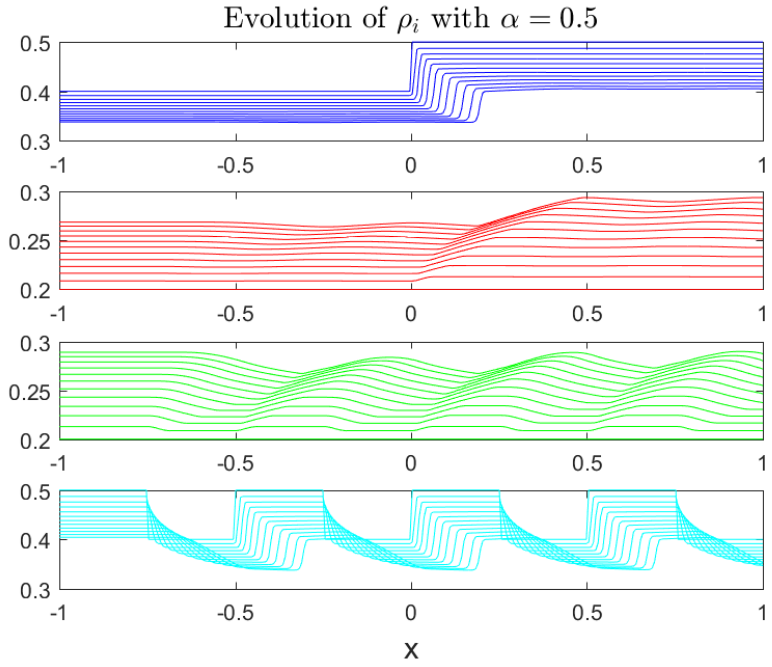

As expected, the increase in α elicits greater change in lane density in fewer timesteps. We see the solution of each lane more quickly approaching a steady, uniform state as t approaches 1.